Effect of MoS_2 Films on Scoring Resistance of Gears

Y. Terauchi
Hiroshima University—Hiroshima, Japan
H. Nadano
M. Kohno
Kure Technical College—Hiroshima, Japan

Introduction

Gears are currently run at high speed and under high load. It is a significant problem to develop lubricants and gears with high load-carrying capacity against scoring. The particles of molybdenum disulfide have been considered to increase the scoring resistance of the gears. The wear characteristics and the scoring resistance of the gears lubricated with MoS_2 paste and MoS_2 powder have been investigated.[1] However, there are few investigations on the performance of the gears coated with MoS_2 film with respect to scoring.

In this report, scoring tests of the gears coated with the MoS_2 film that is about 10 μm thick are carried out with a power-circulating gear machine, and the effect of the MoS_2 film on the scoring resistance and the wear characteristics of the gears are examined. Further, the surface temperature of the gears coated with the MoS_2 film is evaluated by the flash temperature equation of case-hardened gears and the effect of the MoS_2 film on the scoring resistance of the gears is examined from a standpoint of the surface temperature.[2]

Equation of Flash Temperature Rise of Gear Tooth

The equation for calculating the flash temperature rise at the meshing faces of case-hardened gears in which the thermal properties in the surface-hardened layer are different from those in the core of the gear tooth can be rewritten by using the dimensionless parameters as follows:

$$\theta_f = \frac{2\kappa_1 q_0}{\pi K_1 V}\Bigg[\Bigg[4\sqrt{2\pi\beta L}\Bigg[\beta\Big(\frac{1}{3}-\frac{2}{15}\beta\Big) \times\Big\{1+2\sum_{n=1}^{\infty}\alpha^n \exp\Big(-\frac{2n^2\delta^2 L}{\beta}\Big)\Big\} +\Big(\frac{4}{3}-\frac{6}{5}\beta\Big)\delta^2 L\sum_{n=1}^{\infty}\alpha^n n^2\exp\Big(-\frac{2n^2\delta^2 L}{\beta}\Big) -\frac{8}{15}\delta^4 L^2\sum_{n=1}^{\infty}\alpha^n n^4 \exp\Big(-\frac{2n^2\delta^2 L}{\beta}\Big)\Bigg] -4\pi\delta L\sum_{n=1}^{\infty}\alpha^n n\Big\{2\beta-\beta^2+\frac{8}{3}n^2\delta^2 L(1-\beta)-\frac{16}{15}n^4\delta^4 L^2\Big\} \times \mathrm{erfc}\Big(\frac{\sqrt{2L}n\delta}{\sqrt{\beta}}\Big)\Bigg]\Bigg] \quad (1)$$

where $\alpha = (1-\omega)/(1+\omega)$, $\mathrm{erfc}(\gamma) = 1-\mathrm{erf}(\gamma)$,

$$\mathrm{erf}(\lambda) = \frac{2}{\sqrt{\pi}}\int_0^{\lambda}\exp(-\xi^2)d\xi.$$

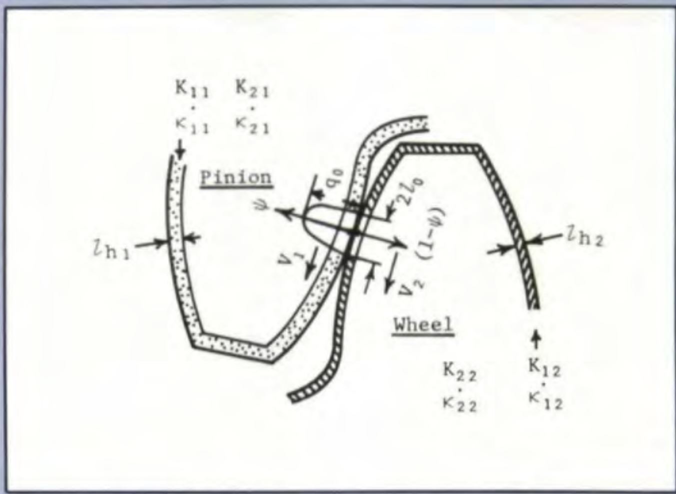

Fig. 1—Schema of mating condition of gear teeth

Fig. 1 shows a schema of the mating condition of the gear teeth. In this figure, the subscripts 1 and 2 relate to the pi-

AUTHORS:

MR. YOSHIO TERAUCHI *is a Professor at the University of Kyoto. He has performed research work in the field of deformation and strength of mating teeth of gears. Terauchi has published numerous papers on rolling contact problems, gear lubrication, scoring, and gear noise. Current research interests include vibration and scoring resistance of bevel gears and performance of the traction drive.*

HIROMASA NADANO *is a Professor at Kure Technical College. Present interests and areas of study include the effect of heat in oil films on tribological phenomena. Academically, he earned a Doctorate in Engineering from the University of Kyoto.*

MR. MASAKI KOHNO *is a lecturer at Kure Technical College. Kohno was awarded a Doctorate in Engineering from Hiroshima University. His major research efforts include scoring and surface roughness.*

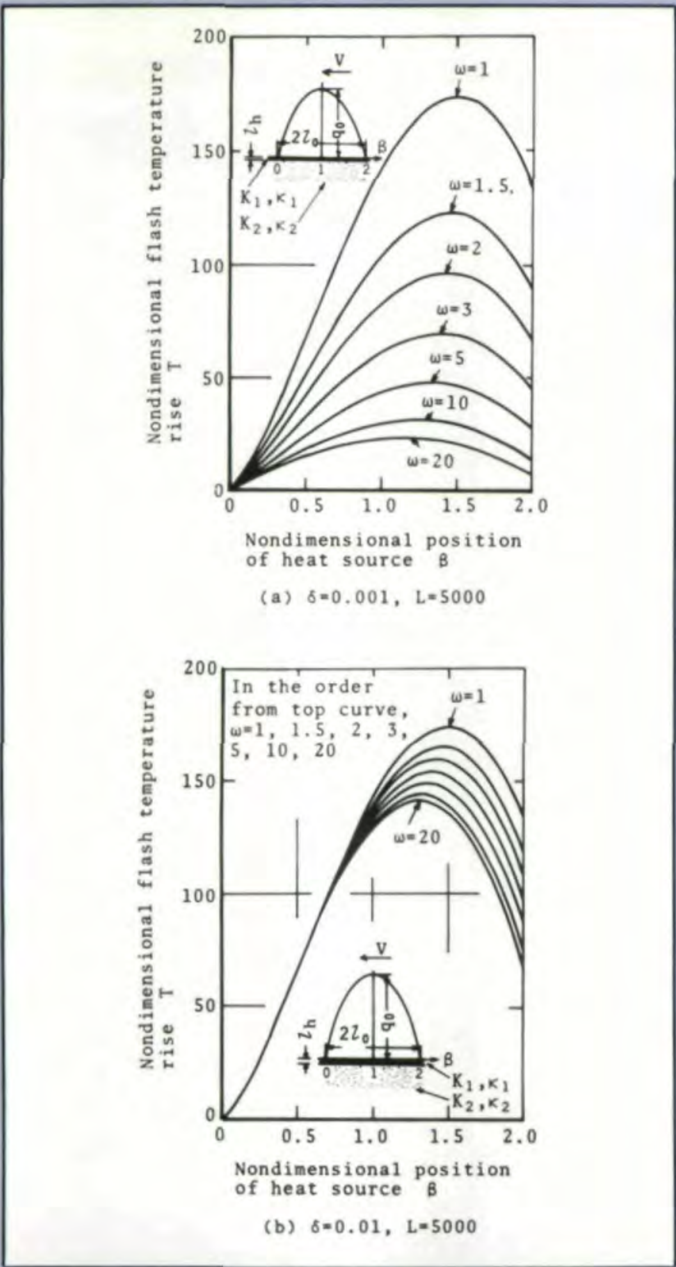

Fig. 2—Relation between nondimensional flash temperature rise and nondimensional position of heat source

nion and the wheel, respectively. The distribution of heat intensity is assumed to be parabolic. Therefore, the value of q_0 is given by,

$$\mu\delta_0 P_n |V_1 - V_2| = 4q_0 l_0/3 \tag{2}$$

The equations of the surface temperature at the meshing faces of the pinion and the wheel are derived from equation (1) as follows:

$$\left.\begin{aligned} \theta_{f_1} &= \frac{2\kappa_{11} q_0}{\pi K_{11} V_1} T_1 \\ \theta_{f_2} &= \frac{2\kappa_{12} q_0}{\pi K_{12} V_2} T_2 \end{aligned}\right\} \tag{3}$$

When the rates of the heat quantity flowing from the conjunctional area into the mating teeth of the pinion and the wheel are expressed by ψ and $1 - \psi$, the surface temperature at the meshing faces of the pinion is equivalent to that of the wheel. Therefore, the value of ψ is given by

$$\psi = \frac{\kappa_{12} K_{11} T_2}{\kappa_{11} K_{12} T_1 V_2/V_1 + \kappa_{12} K_{11} T_2} \tag{4}$$

The surface temperature at the meshing faces is given by

$$\theta_f = \frac{\kappa_{12} T_1 T_2}{\kappa_{11} K_{12} T_1 V_2/V_1 + \kappa_{12} K_{11} T_2} \; \frac{2\kappa_{11} q_0}{\pi V_1} \tag{5}$$

Calculated Results

For example, Figs. 2(*a*) and (*b*) show the relation between the flash temperature rise and the position of the heat source, expressed in terms of the dimensionless parameters T and β, respectively. In this figure, $\omega=1$ indicates that the thermal properties in the surface layer are equivalent to those in the core, and the maximum value of T occurs at $\beta=1.5$. In contrast, $\omega>1$ indicates that the thermal properties in the surface layer are worse than those in the core. The maximum value of T occurs at $1<\beta<1.5$, and the position where the *maximum value of T appears moves toward the vicinity of* the center of the heat source with an increasing value of ω.

Figs. 3(*a*) and (*b*) show the relation between the maximum

(continued on page 22)

Nomenclature

- a = acceleration due to oscillation of gear box, m/s^2
- g = gravitational acceleration = 9.8 m/s^2
- K_1 = thermal conductivity in the surface layer of gear tooth, W/(m K)
- K_2 = thermal conductivity in the core of gear tooth, W/(m K)
- L = nondimensional velocity of heat source = $Vl_0/(2\kappa_1)$
- l_h = thickness of surface layer, m
- l_0 = a half of the band length of Hertzian contact zone, m
- n_1 = rotational speed of pinion, rpm
- P = normal load per unit ball, N
- P_n = normal load per unit face width, N/m
- q_0 = maximum value of heat intensity generated per unit time, W/m^2
- T = nondimensional flash temperature rise = $\pi K_1 V\theta_f/(2\kappa_1 q_0)$
- V = sliding velocity, m/s
- β = nondimensional position of heat source = rV/l_0
- δ = nondimensional thickness of surface layer = l_h/l_0
- δ_0 = load-sharing
- θ_f = flash temperature rise, K
- θ_0 = bulk-temperature, K
- k_1 = thermal diffusivity in the surface layer of gear tooth, m^2/s
- k_2 = thermal diffusivity in the core of gear tooth, m^2/s
- μ = coefficient of friction
- r = time, s
- ω = ratio of thermal contact coefficient of surface layer and core = $(K_2/\sqrt{k_2})/(K_1/\sqrt{k_1})$


THE NEW GLEASON
G-MAXX™
BEVEL GEAR GENERATOR
GLEASON
Visit us at IMTS Booth #6333 McCormick North

THE FIRST TRULY UNIVERSAL BEVEL GEAR GENERATOR EVER MADE

First ever CNC bevel gear generator.

First with two *and* three axis geometries.

First with such superior machine accuracy.

The new Gleason G-MAXX™ 2010 bevel gear generator can give you strong, quiet, high quality gears more productively, more cost efficiently than any other generator ever made.

First In Flexibility

You get three axis geometry for quick, accurate, continuous hobbing. You get a completed gear and pinion in one chucking.

You also get two axis geometry for cutting, grinding and hard finishing by the intermittent face mill process.

The new Gleason G-MAXX generator is designed to either stand alone or function in an automated systems manufacturing environment.

No other generator ever made gives you such choices.

First In Electronics

You program and store your machine settings with Computerized Numeric Control. CNC controls the speed and position for cutter, cradle, workspindle, and sliding base to drastically reduce your set-up time. You can handle smaller, more diverse runs more productively.

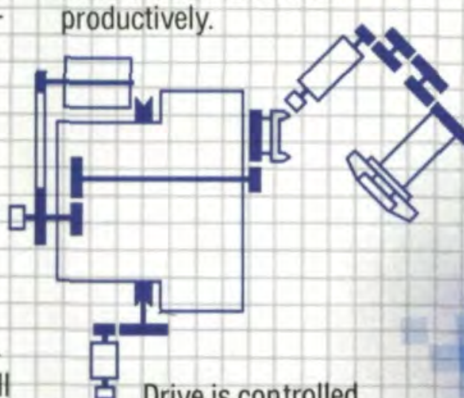

Drive is controlled electronically, not mechanically. Just 14 gears precisely transmit all motion. A shorter drive train maximizes the accuracy and finish of your gear.

First In Tooling

For continuous hobbing, alternate blade design of our exclusive TRI-AC™ cutter allows for more blade groups per head. You can cut far faster than with conventional cutters. Coated front blade surface reduces tool wear so you can cut far more pieces before sharpening. When you do sharpen, coating stays intact. You get a higher quality finish that requires up to 50% less lapping time.

First In Savings

It all adds up. Prime flexibility, CNC control, high accuracy, fast setup, and high quality gear sets can elevate your productivity to greatly diminish your overall cost per piece. And that's the number one benefit to your bottom line.

Ask For A First Cut

We'll be happy to run a comparative manufacturing cost analysis based on your bevel gear needs. Talk to your Gleason representative or call us direct. 716-473-1000. Or write Gleason Works, 1000 University Avenue, Rochester NY 14692 USA. See for yourself all the cost efficient solutions the new Gleason G-MAXX 2010 Generator can bring to you.

GLEASON

G-MAXX and TRI-AC are Trademarks of Gleason Works

CIRCLE A-7 ON READER REPLY CARD

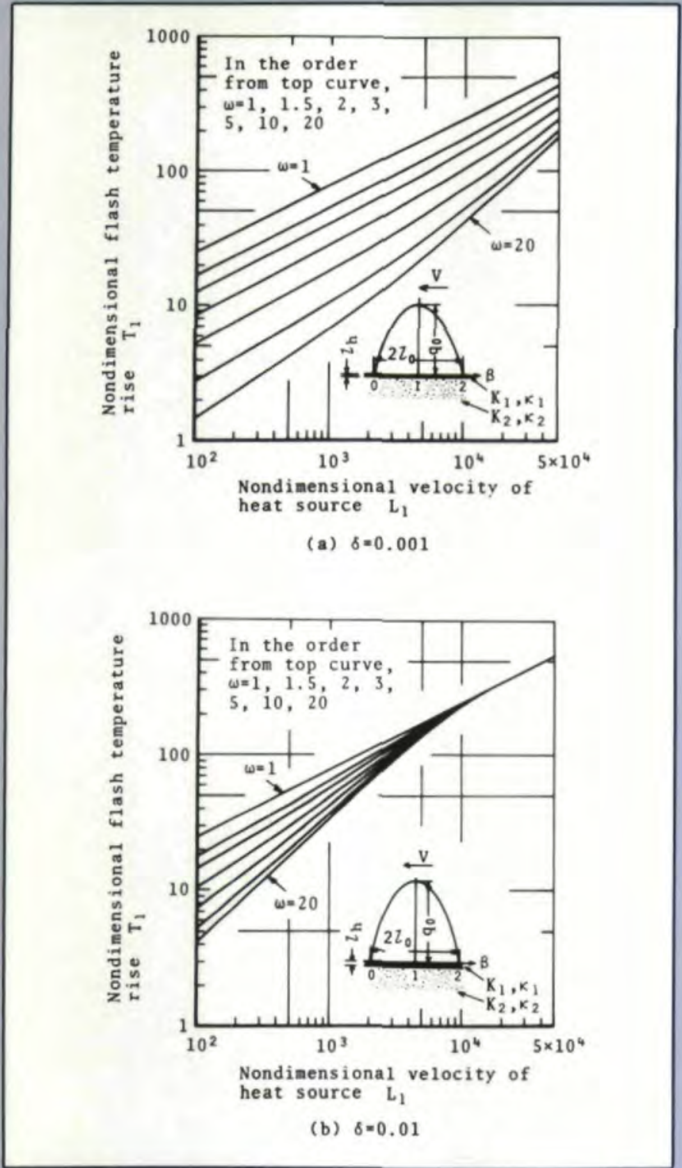

Fig. 3 – Relation between maximum value of nondimensional flash temperature rise and nondimensional velocity of heat source

value of the flash temperature rise and the velocity, expressed in terms of the dimensionless parameters T and L. When the thickness of the surface layer is smaller than the band length of the Hertzian contact zone as shown in Fig. 3(*a*), the effect of ω on the flash temperature rise is significant. In this article, the tooth surface of the gears was coated with the MoS_2 film whose thickness was a little larger than the surface roughness R_{max} of the tooth surface, and the difference between the thermal properties in the surface layer and those in the core is an important problem. The effect of ω on the flash temperature rise decreases with an increasing thickness of the surface layer.

Four Ball Tests

For investigating the seizure load and the frictional characteristics of the balls coated with MoS_2 film, tests have been carried out with a four-ball machine.

Test Balls. The diameter and the average sphericalness of the balls before coating with the MoS_2 film are 19.05 mm and 0.18 μm, respectively. The chemical compositions of ball material are given in Table 1. The balls were normalized at 443 K after quenched from 1173 K. The surface of the balls before coating had a Vickers microhardness of approximately 800 HV. The balls were coated with the MoS_2 film that was about 10μm thick, and the surface roughness of the balls was approximately 9 μm R_{max}.

Table 1 Chemical compositions of ball material

Composition %					
C	Si	P	S	Cr	Mn
0.98	0.32	0.019	0.007	1.40	0.42

Table 2 Combination of ball pairs

		Pair A	Pair B	Pair C	Pair D
MoS_2 coated	Upper ball (Rotating ball)	No	Yes	Yes	No
	Lower balls (Three fixed balls)	No	Yes	No	Yes

Lubricant. The balls were lubricated with number 140 turbine oil (a straight mineral oil without additives) with viscosities of 28×10^{-6} m^2/s at 323 K and 8×10^{-6} m^2/s at 363 K, and the oil temperature was controlled to 293 ± 2 K by the thermostat during all tests. The upper ball was immersed about 1/3 diameter deep into the oil bath.

Experimental Method. The four ball tests were carried out with stepwise increasing loads (the load P was increased by about 40 N increments at 30 s intervals) at a constant sliding velocity 0.29 m/s until the seizure of the balls occurred.

The combination of the balls consists of the four types of the ball pairs as shown in Table 2.

Test Results and Observations

Coefficient of Friction. Fig. 4 shows the relation between the coefficient of friction and the load at the sliding velocity 0.29 m/s. In this figure, the symbol S indicates the incipience of seizure.

Under comparatively low load (P<0.4 kN or the maximum Hertzian stress p_0<3.52 GPa), the coefficient of friction between ball pair A was the largest of all ball pairs, and the coefficient of friction between the balls coated with the MoS_2 film was considerably small. Therefore, the MoS_2 film is considered to play a significant role in decreasing the coefficient of friction. At the incipient stage of seizure, however, the coefficient of friction between the balls coated with the MoS_2 film was approximately equal to that between the balls without it since the MoS_2 film coated on the balls was completely torn out due to wear.

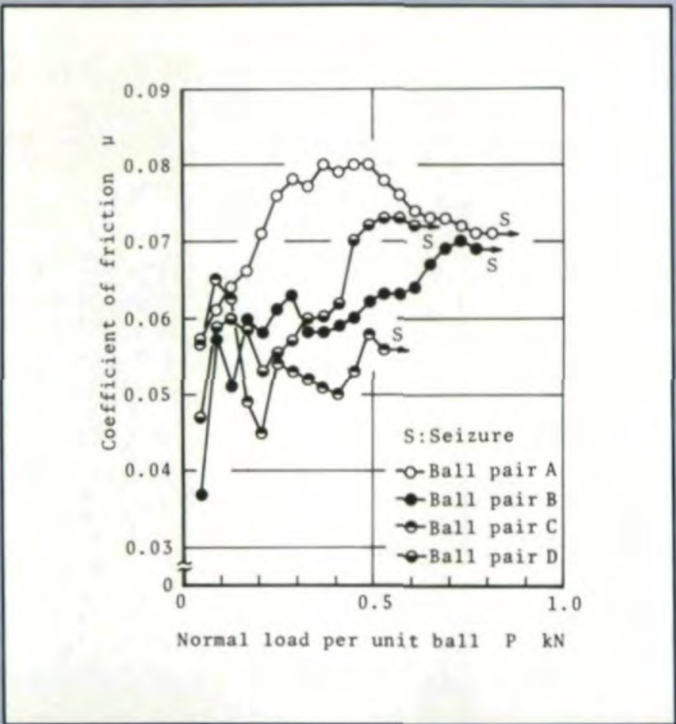

Fig. 4 – Relation between coefficient of friction and load

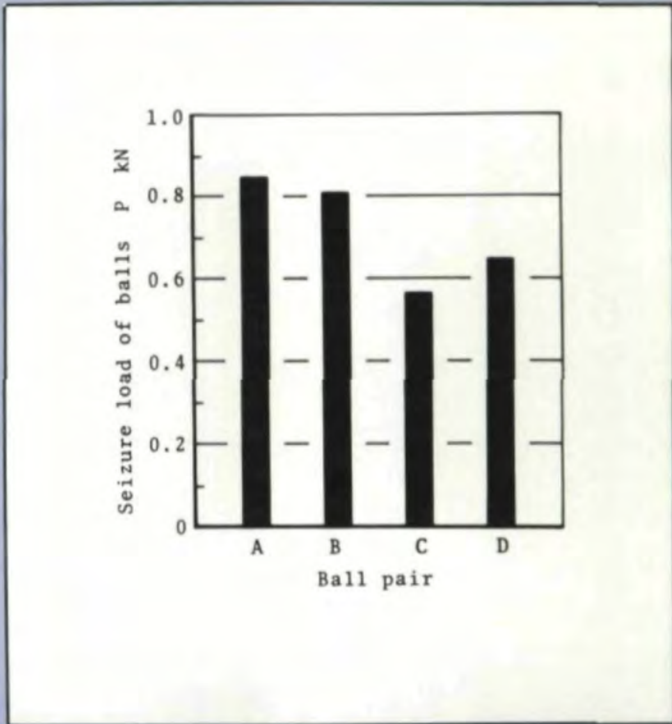

Fig. 5 – Seizure load of balls obtained with four-ball machine

(continued on page 26)

Vertical Hob Sharpener
For straight gash hobs up to 6-in. dia. by 6-in. long. Indexing accuracy for "Class A" tolerances without using index plates.

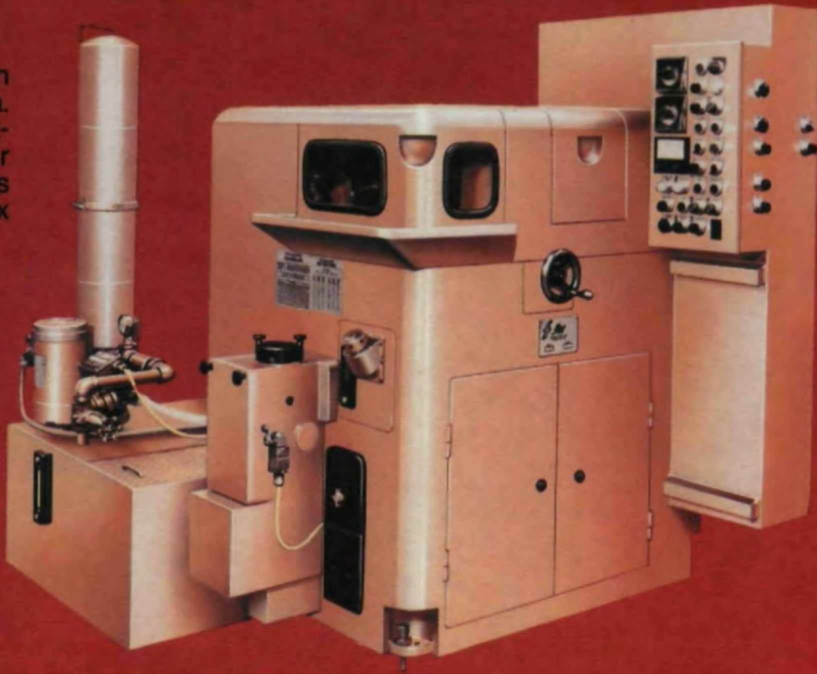

SHARPENING

...the economical and
for your tool sharpen

CNC Drill & Reamer Sharpener
This five axis machine allows users to automatically resharpen tools to their original manufacturing specifications.

These domestically manufactured machines have fully programmable automatic grinding cycles and user needs are fully accommodated in their design. We provide on-site engineering service and training to our customers.

Table 3 Chemical compositions of tooth material

Composition %								
C	Si	Mn	P	S	Ni	Cr	Mo	Cu
0.18	0.28	0.80	0.014	0.019	0.08	0.99	0.16	0.09

Table 5 Combination of gear pairs

		Pair A	Pair B	Pair C	Pair D
MoS_2 coated	Pinion	No	Yes	Yes	No
	Wheel	No	Yes	No	Yes

Table 4 Data for test gears

	Pinion	Wheel
Number of teeth z	18	40
Center distance mm	116	
Pressure angle α_0	20°	
Module m mm	4	
Backlash Sn mm	0.5	
Face width B mm	10	
Effective face width B_f mm	7	
Tooth profile	Standard	
Pitch circle diameter d_0 mm	72	160
Outside diameter d_1 mm	80	168
Contact length mm	19.15	
Contact ratio ε	1.62	
Material	SCM 415H	

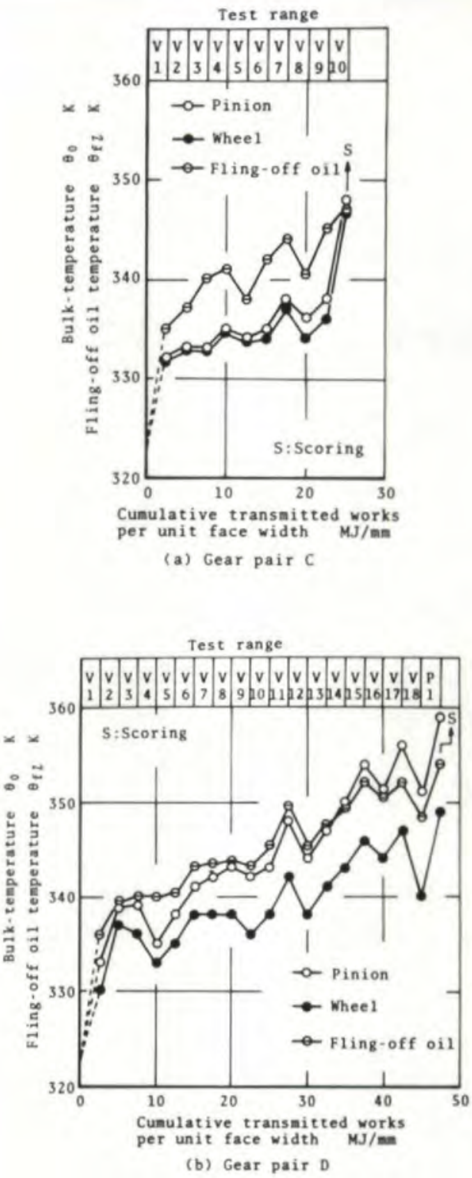

Fig. 6—Variations in bulk-temperature of gear teeth and fling-off oil temperature

Seizure Load. Fig. 5 shows the variation in the seizure load of the balls coated with the MoS_2 film or without it. The seizure load of the balls with ball pair B was not so much different from that with ball pair A, and little effect of the MoS_2 film could be recognized on the seizure load of the balls. Further, with ball pairs C and D, the seizure load of the balls was smaller than that with ball pair A, and it rather decreased due to the coating of the MoS_2 film.

Gear Tests

Scoring tests of the gears coated with MoS_2 film were run with a power-circulating gear machine. The effect of the MoS_2 film on the scoring resistance of the gears was investigated.

Test Gears. The test gears were made of chrome-molybdenum steel and case-hardened by gas-carburizing. The chemical compositions of tooth material are shown in Table 3. The working surface of the gears had a Vickers microhardness of approximately 720 HV. The gears were ground by a gear grinding machine as shown in Table 4. The single-pitch error and the tooth profile error of the gears were approximately 2 μm before coating with the MoS_2 film. The accuracy of the tooth profile of the gears before coating was of zero class, according to the Japanese Industrial Standard JIS B 1702. The surface roughnesses along the tooth trace of the pinion and the wheel before coating were about 2 μm R_{max}.

The combination of the gears consists of the four types of the gear pairs as shown in Table 5. The gear teeth were coated

Experimental Method. The scoring tests were carried out with the MoS_2 film that was about 10 μm thick after grinding, and the surface roughness after coating was approximately 9 μm R_{max}.

Lubricant. The test gears were lubricated with the same oil used for the four ball tests. The oil was sprayed onto the meshing faces at a rate of 0.6 L/min. The oil temperature was controlled to 323±2 K by the thermostat during all tests.

Table 6 (a) Speed data

Speed range	V-1	V-2	V-3	V-4	V-5	V-6	V-7	V-8	V-9	V-10	V-11	V-12	V-13	V-14	V-15	V-16	V-17	V-18
Rotational speed of pinion n_1 rpm	2000	2310	2644	3001	3381	3783	4208	4655	5125	5618	6133	6671	7231	7814	8420	9048	9699	10372
Peripheral velocity m/s	7.5	8.7	10.0	11.3	12.7	14.3	15.9	17.6	19.3	21.2	23.1	25.2	27.3	29.5	31.7	34.1	36.6	39.1
Cumulative transmitted works * MJ/mm	2.5	5.0	7.5	10.0	12.5	15.0	17.4	19.9	22.4	24.9	27.4	29.9	32.4	34.9	37.4	39.9	42.4	44.9

* The cumulative transmitted works are defined as the sum of the transmitted works per unit face width at the respective test ranges.

Table 6 (b) Load data

Load range	P-1	P-2	P-3	P-4	P-5	P-6	P-7	P-8	P-9	P-10
Tooth load Pn N/mm	278	290	302	314	327	339	352	364	377	390
Cumulative transmitted works MJ/mm	47.5	50.2	53.0	55.9	59.0	62.2	65.4	68.8	72.4	76.0

at stepwise increasing pinion speeds from V-1 to V-18 as shown in Table 6(*a*). The increment of the calculated value of the flash temperature rise was the same for the respective speed ranges under a constant load of $P_n = 266$ N/mm. When surface failure by scoring was not observed up to the speed range V-18, the tests were continued with stepwise increasing loads at a constant pinion speed of $n_1 = 10372$ rpm as shown in Table 6(*b*). The increment of the flash temperature rise per unit load range corresponds to that of the flash temperature rise per unit speed range.

The tests were run until the total number of pinion revolutions reached 4.4×10^4 at the respective ranges.

Scoring was detected by the following methods: (*a*) visual inspection of the tooth faces; (*b*) measurement of the surface roughnesses along the tooth trace and the tooth profile of the gears; (*c*) measurements of the bulk-temperature of the mating teeth and the fling-off oil temperature; (*d*) measurement of the acceleration due to oscillation of the gear box.

To measure the surface roughness along the tooth profile, the feeler set on the tooth profile testing machine was replaced with a thin cantilever in which a diamond needle was attached to the end of a plate spring that was 0.2 mm thick. The surface roughness was detected with a semiconductor strain gage that was attached to the root of the cantilever.

The bulk-temperature of the mating teeth was measured by pressing a contact-type thermister thermometer against the side of the tooth just after the test machine was stopped. Therefore, the bulk-temperature measured was considered to be a little lower than that in running.

The fling-off oil temperature was measured by thermocouples set up at a position opposite the mating position of the pinion. The distance between the hot junction of the thermocouples and the tip of the pinion was approximately 1 mm.

The acceleration due to oscillation of the gear box was measured by a piezoelectric accelerometer attached to the side of the test gear box.

The measurement of the acceleration due to oscillation was started 1 minute before each end of the respective test ranges, and the acceleration was recorded on the magnetic tape of a data recorder (characteristics of FM : 0 ~ 10 kHz) for about 30 s.

Test Results and Observations

Bulk-Temperature of Gear Tooth and Fling-Off Oil Temperature. For example, Fig. 6 shows the variations in the bulk-temperature of the gear teeth and the fling-off oil temperature with gear pair C (a pinion with the MoS_2 film and a wheel without it) and gear pair D (a pinion without the MoS_2 film and a wheel with it) until surface failure is caused by scoring. In this figure, the symbol S indicates the incipience of surface failure by scoring.

The values of the thermal properties of tooth material and MoS_2 material are shown in Table 7. As evident from equation (4), when the MoS_2 film-coated gear teeth with low thermal properties mate with the gear teeth without it, the rate of the frictional heat flowing into the meshing faces of the gears with the MoS_2 film is less than the gears without it. Thus, the bulk-temperature of the mating teeth coated with the MoS_2 film becomes lower than that of the gears without it.

With gear pair C, the difference between the bulk-temperatures of the mating teeth of the pinion and the wheel was insignificant, and the effect of the MoS_2 film could be recognized on the bulk-temperature of the mating teeth. The bulk-temperature suddenly increased by about 10 K at the incipience of surface failure by scoring. On the other hand, the fling-off oil temperature was higher than the bulk-temperature of the gear teeth.

With gear pair D, in contrast, the difference between the

Table 7 Values of thermal properties of tooth material[2] and MoS_2 material[3]

Material	Thermal conductivity K W/(m K)	Thermal diffusivity κ m^2/s
SCM 415H (373 K)	24	6.67×10^{-6}
MoS_2 (373 K)	0.14	6.88×10^{-8}

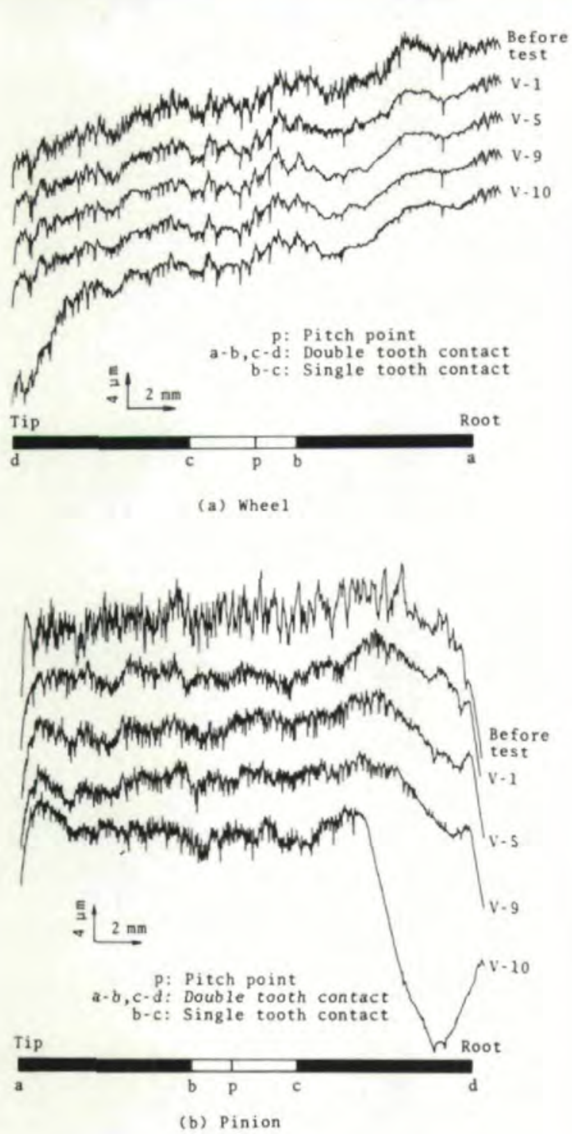

Fig. 7 – Variation in surface roughness along tooth profile with gear pair C

bulk-temperatures of the mating teeth of the pinion and the wheel significantly increased with an increasing test range, and the bulk-temperatures of the pinion was approximately 10 K higher than that of the wheel at the incipience of surface failure by scoring. On the other hand, the fling-off oil temperature was not so much different from the bulk-temperature of the pinion.

Surface Roughness. The variation in the surface roughness of the tooth surface along the tooth profile at the center of the face width with gear pair C is shown in Fig. 7. The variation in the surface roughness of the wheel before surface failure is caused by scoring was considerably small. On the other hand, the depth of a hollow occurring in the vicinity of the root of the pinion considerably increased with an increasing test range. The surface roughness along the tooth profile of the pinion coated with the MoS_2 film before tests was 8 μm R_{max}, and the surface roughness at the speed range V-1 was 3 μm R_{max} since the MoS_2 film coated on the tooth surface was torn out due to wear. However, the variation in the surface roughness after V-5 was considerably small.

A destructive surface failure by scoring occurred in the vicinity of the meshing position when the tip of the wheel mated with the root of the pinion. The EHD film thickness, calculated by Dowson's formula, at the meshing position at which destructive surface failure by scoring was observed, is 0.33 μm at V-10. Since the value of λ[4], defined as the ratio of the film thickness to combined surface texture, is approximately 0.9, the tests were run under mixed lubricating conditions.

For example, Fig. 8 shows the variation in the surface roughness of the tooth surface along the tooth trace in the vicinity of the tip of the wheel with gear pair D. The thickness of the MoS_2 film coated on the tooth surface of the wheel decreased by approximately 8 μm at V-1. After the test range exceeded V-11, the variation in the thickness of the MoS_2 film was considerably small. Surface failure by scoring occurred at the load range P-1, and a part of the base metal

Fig. 8 – Variation in surface roughness along tooth trace in the vicinity of tip of wheel gear pair D

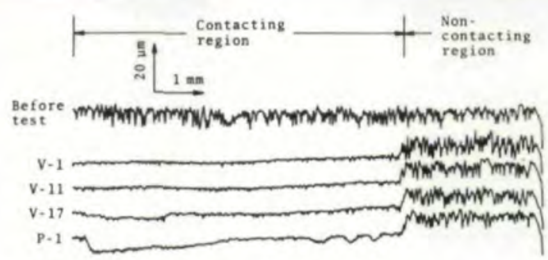

Fig.8 Variation in surface roughness along tooth trace in the vicinity of the tip of wheel with gear pair D

Fig. 9 – Electron micrographs obtained with scanning X-ray microanalyzer at tip of wheel with gear pair D

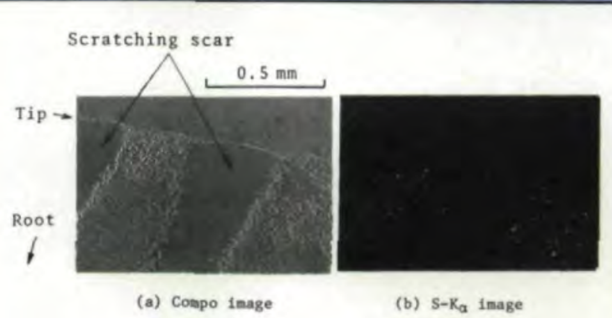

(continued on page 30)

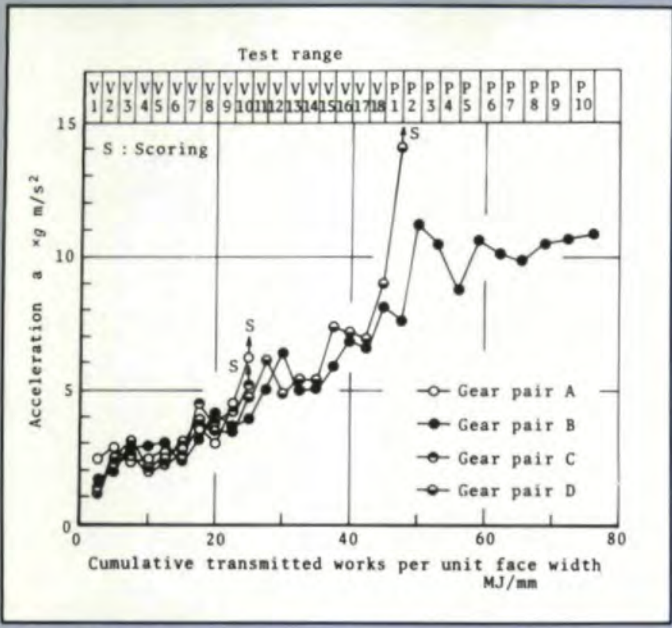

Fig. 10 – Variation in acceleration due to oscillation of gear box

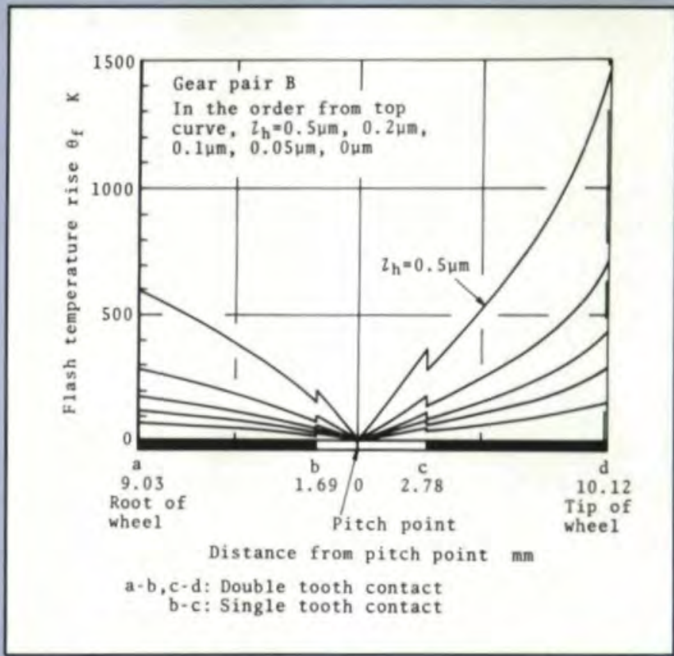

Fig. 11 – Variation in flash temperature rise at successive meshing positions along the line of action

of the gear tooth was exposed on the tooth surface.

Fig. 9 shows electron micrographs of the compo image and the *S-Kα* image which were obtained with a scanning X-ray microanalyzer at the tip of the gear tooth of the wheel with gear pair D. The MoS_2 film at the tip of the wheel was torn out due to wear, and the tooth surface was considerably smooth. However, the particles of sulfur were present at the tooth surface at which the scratching scar did not occur. From this photograph, it can be found the MoS_2 film is formed enough at the meshing faces at the incipience of surface failure by scoring, and the film significantly affects the scoring resistance of the gears.

Acceleration of Gear Box. Fig. 10 shows the variation in the acceleration due to oscillation of the gear box. The acceleration increased with an increasing test range. With gear pair D, the acceleration of the gear box suddenly increased by about 5*g* at P-1, and the incipience of surface failure by scoring could be detected by means of the measurement of the acceleration due to oscillation of the gear box.

Surface Temperature and Scoring Resistance. Fig. 11 shows the variation in the flash temperature rise at the successive meshing positions along the line of action, calculated by equations (1-5) under the following conditions: number of pinion teeth $z_1 = 18$, number of wheel teeth $z_2 = 40$, module $m = 4$ mm, face width $B_f = 7$ mm, backlash $S_n = 0.5$ mm, clearance coefficient $C_e = 0.25$, tooth load $P_n = 266$ N/mm, pinion speed $n_1 = 6000$ rpm.

The surface roughness at the meshing faces and the bulk-temperature of the gear teeth were assumed to be zero. The load-sharing was calculated from the elastic deformation of teeth. In this calculation, Young's modulus E and Poisson's ratio v of tooth material are assumed to be E = 206 GPa and $v = 0.3$, respectively. The coefficient of friction can be given by $\mu = 0.1\ V_p^{-0.2}$, where V_p is the peripheral velocity (m/s) at the pitch point.[5] Since the thickness of the MoS_2 film coated on the tooth surface is very small, it can be assumed that the mechanical properties of the MoS_2 film do not affect the band length of the Hertzian contact zone and the radius of relative curvature of the tooth surface at meshing position of the gears.

From this figure, it can be found that the flash temperature rise considerably increases with an increasing thickness of the MoS_2 film, and the effect of the MoS_2 film on the flash temperature rise is significant.

Fig. 12 shows the test range and the cumulative transmitted works per unit face width at the incipience of surface failure

Fig. 12 – Test range and cumulative transmitted works per unit face width at incipience of surface failure by scoring

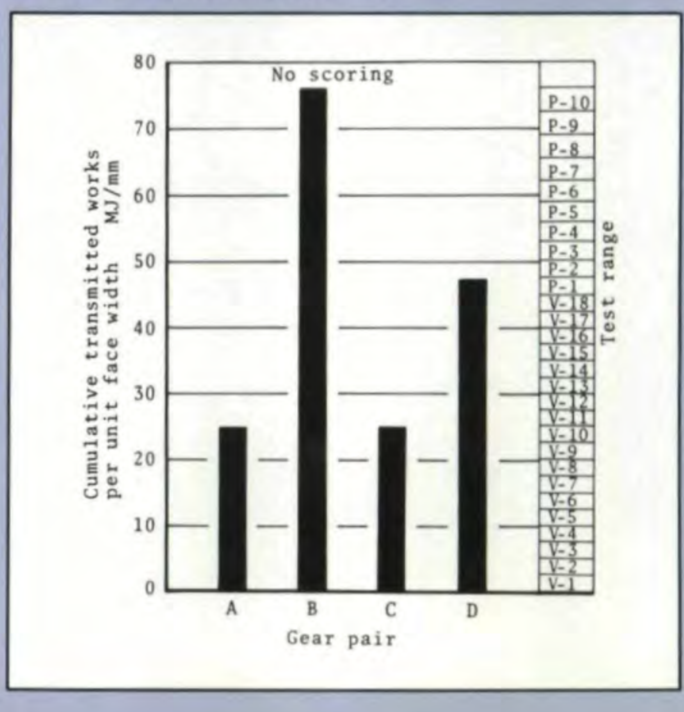

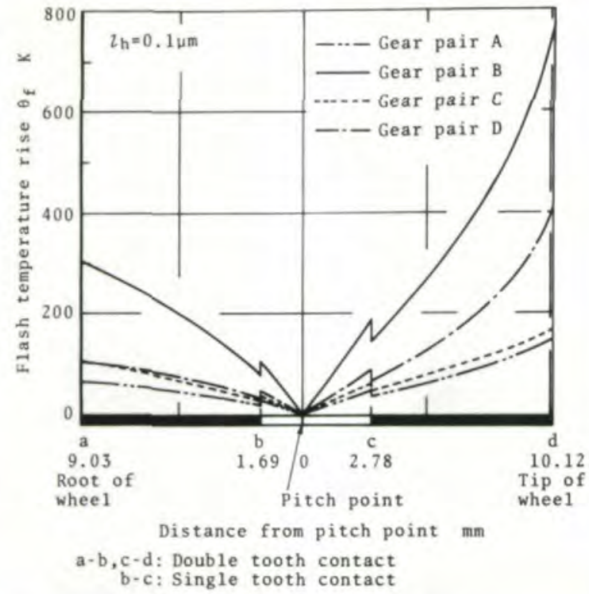

Fig. 13 – Variation in flash temperature rise at successive meshing positions along the line of action at incipience of surface failure by scoring

by scoring. With gear pair B, the tests were stopped at P-10 because the scoring resistance of the gears exceeds the load carrying capacity of the test machine. From this figure, it can be seen that gear pair B provides the highest scoring resistance of all test gears, and the MoS_2 film plays a significant role in increasing scoring resistance of the gears. Further, the scoring resistance of the gears with gear pair D is larger than that of the gears with gear pair C, and the MoS_2 film coated on the tooth surface of the wheel is more effective for the scoring resistance of the gears than that coated on the tooth surface of the pinion.

Fig. 13 shows the variation in the flash temperature rise at the successive meshing positions along the line of action at the incipience of surface failure by scoring. The flash temperature rise is calculated by substituting the tooth load, the pinion speed, the coefficient of friction and the thickness of the MoS_2 film into equations (1-5). From the observation of the sectional plane cut along the tooth profile, it was found that a part of the MoS_2 film was torn out due to wear and the thickness of the film was not uniform on the tooth surface. However, the thickness of the film was assumed to be $l_h = 0.1\ \mu m$.

From this figure, it is interesting to note that the maximum value of the flash temperature rise occurs at the meshing position where the tip of the wheel mates with the root of the pinion, and the position well agrees with the position at which destructive failure by scoring was observed.

The critical surface temperature for scoring of the gears is shown in Table 8. The critical surface temperature for scoring of the gears with gear pairs B and D is extremely high because the flash temperature rise of the gears is calculated under the assumptions that the MoS_2 film is uniformly distributed on the tooth surface and the coefficient of friction between the gear pairs coated with the MoS_2 film is equivalent to that between the gear pairs without it. However, a part of the MoS_2 film coated on the tooth surface was torn out just before surface failure was caused by scoring, and the thickness of the film was not uniform on the tooth surface. Further, according to the test results obtained with the four ball tests, the coefficient of friction between the balls coated with the MoS_2 film was smaller than that between the balls without it.

From the above cited facts, it can be considered that the critical surface temperature for scoring of the gears coated with the MoS_2 film is lower that the value shown in Table 8. However, the scoring resistance of the gears coated with the MoS_2 film is considerably large, and the MoS_2 film is considered to play a significant role in increasing scoring resistance of the gears.

Conclusions

Calculated surface temperatures and the experimental results obtained with four ball tests and gear tests with respect to the effect of the MoS_2 film on the scoring resistance of the gears are summarized as follows:

1. When the thickness of the surface layer is smaller than the band length of the Hertzian contact zone, the effect of the thermal properties in the surface layer on the flash temperature rise is significant, and the difference between the

Table 8 Critical surface temperature for scoring of gears

Gear pair	R_{rms} (a) μm	Bulk-temperature (b) θ_0 K	Maximum flash temperature rise θ_f K	Critical surface temperature (c) θ_{cr} K
A	0.33	340	148	540
B (d)	(0.37)	(351)	(770)	(1438)
C	0.36	337	167	570
D	0.48	346	411	1007

(a) R_{rms} is the mean value of the root mean square roughness along the tooth trace of the pinion and wheel just before scoring.
(b) θ_0 is the mean value of the bulk-temperature of the gear teeth of the pinion and wheel just before scoring.
(c) $\theta_{cr} = \theta_0 + \theta_f \times 1.27/(1.27 - R_{rms})$ [6]
(d) The numerals in parentheses are the value of the variables at P-10.

thermal properties in the surface layer and those in the core is an important problem.

2. Under comparatively low load (P<0.4 kN), the coefficient of friction between the balls coated with the MoS_2 film was 2/3 of that between the balls without it.

3. The scoring resistance of the gears coated with the MoS_2 film is considerably large, and the MoS_2 film plays a significant role in increasing scoring resistance of the gears. The development of the gears of which the load-carrying capacity against scoring is considerably large could be made.

References

1. BARTZ, W. J., "Some Investigations on the Influence of Particle Size on the Lubricating Effectiveness of Molybdenum Disulfide," *ASLE Trans.*, Vol. 15, 1972, pp. 207-215.
2. TERAUCHI, Y., MIYAO, Y., and NADANO, H., "On the Flash Temperature Rise of the Tooth Surface of Surface-Hardened Gears," *Bulletin of the JSME*, Vol. 16, No. 99, 1973, pp. 1443-1456.
3. YAMAMOTO, T., and HANADA, H., "Manufacturing Process of Solid Lubricants," *Jour. Japan Soc. Lub., Engrs.* (in Japanese), Vol. 27, No. 4, 1982, pp. 233-237.
4. WELLAUER, E. J., and HOLLOWAY, G. A., "Application of EHD Oil Film Theory to Industrial Gear Drives," ASME *Journal of Engineering for Industry*, Vol. 98, No. 2, May 1976, pp. 626-634.
5. *ISO TC60/WG6*, "Calculation of Scoring Resistance," Dutch-Swiss draft, May 1977.
6. TERAUCHI, Y., and NADANO, H., "Effect of Tooth Profile Modification on the Scoring Resistance of Spur Gears," *Wear*, Vol. 80, 1982, pp. 27-41.

This article was presented previously at the ASME Design Engineering Conference, October 1984. Paper No. 84-DET-59.